ORIGINAL ARTICLE

Hiroshi Yoshihara · Yoshitaka Kubojima

Measurement of the shear modulus of wood by asymmetric four-point bending tests

Received: December 8, 2000 / Accepted: February 28, 2001

Abstract We conducted asymmetric four-point bending tests of wood and obtained the shear moduli on the basis of Timoshenko's theory of bending. Akamatsu (Japanese red pine, *Pinus densiflora* D. Don) and shioji (Japanese ash, *Fraxinus spaethiana* Lingelsh.) were used for the tests. Asymmetric four-point bending tests were undertaken by varying the depth/span ratios; and Young's modulus and the shear modulus were calculated by Timoshenko's bending theory. Independent of the asymmetric bending tests, we also conducted three-point bending tests, free-free-flexural vibration tests, and numerical calculations by the finite element method. Young's and shear moduli obtained by these methods were compared with those derived from the asymmetric bending tests. Based on these comparisons, we concluded that the shear modulus can be properly obtained by the asymmetric four-point bending tests when the span is 20 times larger than the depth.

Key words Shear modulus · Asymmetric four-point bending test · Timoshenko's beam theory · Depth/span ratio

Introduction

To develop a design methodology for wood and wood products, deformation by shear makes the shearing properties one of the important parameters in the design processes. In the beam with an I-shaped cross section, for example, the deflection by shear is significant because of the slenderness along the neutral axis. If beams designed without considering the shearing deflection are used for flooring materials, the deformation of the floor is so serious it causes vibrations from which the resident may suffer. Thus, the shear modulus should be measured properly to predict the magnitude of the shearing deformation.

Various testing methods are available to determine the shear modulus, such as the torsion test,[1,2] the Iosipescu test,[3,4] and the tension or compression test of a 45° off-axis specimen.[1] These tests, however, have their drawbacks. The torsion and Iosipescu tests require special equipment. For the tension or compression test of the off-axis specimen, the specimen's geometry is restricted. If these testing methods were simpler and more convenient, a reliable engineering database for shearing properties, including the shear modulus, could be developed. The bending test under varying the span/depth ratios is simpler than these methods.

In previous studies the shear moduli of several wood species were measured by three-point bending tests based on Timoshenko's bending theory. The theoretical shear modulus was estimated to be smaller than the real value because of the extra deflection that cannot be predicted by the theoretical construct. To obtain the proper shear modulus value, the original Timoshenko equation was modified taking into consideration the test results and numerical analyses.[5,6] Nevertheless, it is more convenient that the shear modulus is properly measured without modifying the original equation because several experimental conditions (e.g., the radius of the loading nose and the measurement of deflection) influence the modification.[6,7] The asymmetric four-point bending test whose detail is mentioned below is a promising method for obtaining the shear modulus because the deflection produced by the shearing force is emphasized. In this study we conducted asymmetric four-point bending tests on two wood species and examined their validity by comparing the results with those obtained by other testing methods.

Theories

Figure 1a outlines the asymmetric four-point bending test. The distance between the outer spans is l, and the directions

H. Yoshihara (✉)
Faculty of Science and Engineering, Shimane University, Nishikawazu-cho 1060, Matsue, Shimane 690-8504, Japan
Tel. +81-852-32-6508; Fax +81-852-32-6123
e-mail: yosihara@riko.shimane-u.ac.jp

Y. Kubojima
Forestry and Forest Products Research Institute, Tsukuba 305-8687, Japan

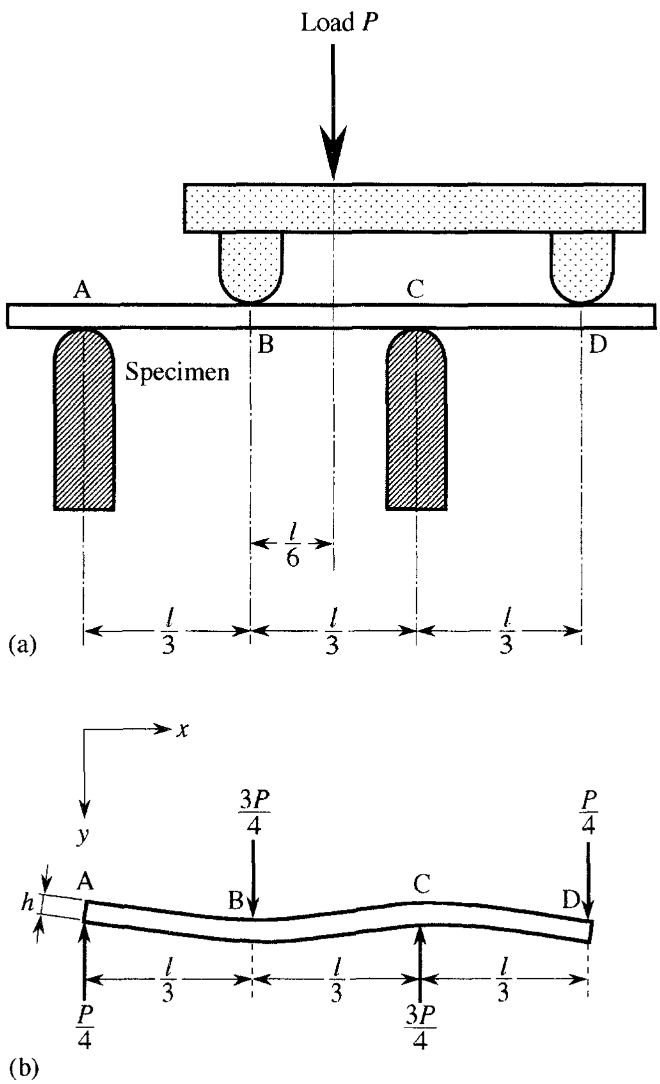

Fig. 1. Asymmetric four-point bending test and the beam subjected to the lateral forces

parallel and perpendicular to the length are defined as x and y, respectively. The specimen is supported at the point of $x = 0$ and $2l/3$, which are denoted A and C, respectively; and the load is applied at points $x = 2l/3$ and l, denoted B and D, respectively. When the displacements of B and D are similar, the total load of P is divided into $3P/4$ and $P/4$ for B and D, respectively, whereas the reaction forces at A and C are $P/4$ and $3P/4$, respectively. Figure 1b shows the beam asymmetrically subjected to the lateral forces. Under this loading condition, the bending equation is derived by the elementary bending theory as follows.[8]

$$M = E_x I \frac{d^2y}{dx^2} = \begin{cases} -\frac{1}{4}Px & \left(0 \le x \le \frac{l}{3}\right) \\ \frac{1}{2}Px - \frac{1}{4}Pl & \left(\frac{l}{3} \le x \le \frac{2l}{3}\right) \\ -\frac{1}{4}Px + \frac{1}{4}Pl & \left(\frac{2l}{3} \le x \le l\right) \end{cases} \tag{1}$$

where M is the bending moment, E_x is Young's modulus in the length direction, and I is the moment of inertia. By solving this equation, the displacement line caused by the bending moment, y_b, is given when $(x, y_b) = (0, 0)$ as:

$$y_b = \begin{cases} \frac{P}{E_x I}\left(-\frac{1}{24}x^3 + \frac{5}{432}l^2 x\right) & \left(0 \le x \le \frac{l}{3}\right) \\ \frac{P}{E_x I}\left(\frac{1}{12}x^3 - \frac{1}{8}lx^2 + \frac{23}{432}l^2 x - \frac{1}{216}l^3\right) & \left(\frac{1}{3} \le x \le \frac{2l}{3}\right) \\ \frac{P}{E_x I}\left(-\frac{1}{24}x^3 + \frac{1}{8}lx^2 - \frac{49}{432}l^2 x + \frac{7}{216}l^3\right) & \left(\frac{2l}{3} \le x \le l\right) \end{cases} \tag{2}$$

The equation represents that the beam is supported by A and C, and that the displacements of B and D are similar to each other.

During bending the displacement caused by the shearing force, denoted y_s, is always produced; and the slope of the deflection line by the shearing force dy_s/dx is represented by Timoshenko's bending theory as:[8]

$$\frac{dy_s}{dx} = \frac{sV}{G_{xy}A} \tag{3}$$

where G_{xy} is the shear modulus in the xy-plane, V is the shearing force, A is the cross-sectional area of the beam, and s is Timoshenko's shear factor. This factor is 1.5 for a beam with a rectangular cross section when it is defined as the maximum/average shear stress ratio, whereas it is derived as 1.2 by calculating the strain energy. The shearing force is obtained by differentiating the bending moment by x. Hence, from Eqs. (1) and (3), dy_s/dx is represented as follows:

$$\frac{dy_s}{dx} = \frac{s}{G_{xy}A}\frac{dM}{dx} = \begin{cases} -\frac{s}{4G_{xy}A}P & \left(0 \le x \le \frac{l}{3}\right) \\ \frac{s}{2G_{xy}A}P & \left(\frac{l}{3} \le x \le \frac{2l}{3}\right) \\ -\frac{s}{4G_{xy}A}P & \left(\frac{2l}{3} \le x \le l\right) \end{cases} \tag{4}$$

The value of y_s is 0 in $x = 0$ and l; hence

$$y_s = \begin{cases} -\frac{s}{4G_{xy}A}Px & \left(0 \le x \le \frac{l}{3}\right) \\ \frac{s}{2G_{xy}A}Px - \frac{s}{4G_{xy}A}Pl & \left(\frac{l}{3} \le x \le \frac{2l}{3}\right) \\ -\frac{s}{4G_{xy}A}Px + \frac{s}{4G_{xy}A}Pl & \left(\frac{2l}{3} \le x \le l\right) \end{cases} \tag{5}$$

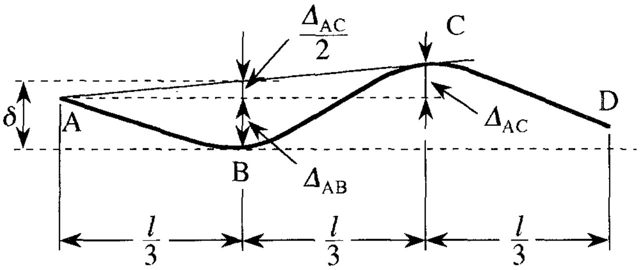

Fig. 2. Definition of vertical displacements in asymmetric four-point bending

Figure 2 illustrates the vertical displacement with asymmetric bending. In the elastic strain range, the vertical displacement is much smaller than the span, and the deflection at point B, denoted δ, is approximated as follows:

$$\delta = \Delta_{AB} + \frac{1}{2}\Delta_{AC} \tag{6}$$

where Δ_{AB} and Δ_{AC} are the vertical displacements of points A and C, respectively, with respect to point B. By substituting $x = l/3$ and $2l/3$ into Eqs. (2) and (5), Δ_{AB} and Δ_{AC} are calculated as:

$$\Delta_{AB} = \frac{Pl^3}{432E_xI} + \frac{sP}{12G_{xy}A} \tag{7}$$

and

$$\Delta_{AC} = \frac{sP}{12G_{xy}A} \tag{8}$$

When the depth and breadth of the specimen are denoted h and b, respectively, δ is derived from Eqs. (6), (7), and (8) as:

$$\delta = \frac{Pl^3}{432E_xI} + \frac{sP}{8G_{xy}A} = \frac{Pl^3}{36E_xbh^3}\left\{1 + 4.5s\frac{E_x}{G_{xy}}\left(\frac{h}{l}\right)^2\right\} \tag{9}$$

According to the elementary bending theory, the effect of shearing force is ignored, and the second term in the braces of Eq. (9) vanishes. When Young's modulus based on the elementary bending theory is given by E_s, the deflection δ is represented as follows:

$$\delta = \frac{Pl^3}{432E_sI} = \frac{Pl^3}{36E_sbh^3} \tag{10}$$

The following relation is obtained from Eqs. (9) and (10).

$$\frac{1}{E_s} = \frac{1}{E_x} + 4.5\frac{s}{G_{xy}}\left(\frac{h}{l}\right)^2 \tag{11}$$

This equation indicates that the effect of shearing force during asymmetric four-point bending is 4.5 times that with three-point bending.[5–8] With three-point bending, the extra deflection that cannot be predicted by Timoshenko's bending theory is so marked the shear modulus calculated by Timoshenko's equation tends be smaller than the real value. The emphasized shearing effect during asymmetric bending, however, might obscure the extra deflection.

Experiment

Materials and testing procedures

Akamatsu (Japanese red pine, *Pinus densiflora* D. Don) and shioji (Japanese ash, *Fraxinus spaethiana* Lingelsh.) were used for the tests. The density of akamatsu was 0.66 g/cm^3, whereas that of shioji was 0.58 g/cm^3. Specimens were conditioned at 20°C and 65% relative humidity before and during the tests.

Six specimens were used for each species. These 12 specimens initially had the dimensions of 10 mm (tangential) depth, 20 mm (radial) breadth, and 350 mm (longitudinal) length. Young's and shear moduli corresponding to the 12 specimens were determined by the flexural vibration, asymmetric four-point bending, and three-point bending tests. The depth of the specimen was then decreased to 5 mm by a planer, and Young's modulus and the shear modulus for each specimen were obtained by the asymmetric four-point and three-point bending tests. Thus, the five values for Young's modulus and the five values for the shear modulus were derived from one specimen.

Asymmetric four-point bending tests

Asymmetric four-point bending tests were undertaken by the following procedure. The specimen was settled on supports that correspond to points A and C in Fig. 1a. The distances between supports were 318, 222, 183, 159, 141, 129, 120, 111, 105, and 99 mm. By determining the distance between the supports as above, the value of $(h/l)^2$ varied from approximately 0.001 to 0.01 at an interval of 0.001 and a depth of 10 mm, whereas it varied from approximately 0.0002 to 0.0025 at an interval of 0.00025 and a depth of 5 mm. With loading noses whose radii were 15 mm, a vertical load was applied asymmetrically at points B and D in Fig. 1a at a loading speed of 1 mm/min. To reduce the extra deflection produced by the stress concentration around the loading noses and the machine compliance, the deflection was measured at the bottom of the loading point, which corresponds to point B in Fig. 1a by the cantilever-type displacement gauge. The load was carefully applied so as not to exceed the elastic limit of the specimen, which was used repeatedly in this experiment. From the load (P)-displacement (δ) relation, the apparent Young's modulus E_s corresponding to the depth/span ratio h/l was calculated by Eq. (10). The $1/E_s$–$(h/l)^2$ relation was then regressed into Eq. (11) by the method of least squares, and Young's modulus E_x and the shear modulus G_{xy} were obtained.

Three-point bending tests

Three-point bending tests had been conventionally undertaken to determine the shear modulus of wood.[5–7,9,10] Here we conducted the three-point bending tests with the same specimens used for the asymmetric bending tests and compared the obtained shear moduli with those obtained by the asymmetric bending tests. The testing conditions such as span lengths, loading speed, and loading nose radius were similar to those of the asymmetric bending tests. The load was applied at the center of the specimen, and the deflection was measured by the displacement gauge set behind the loading point. Based on the load-deflection diagram, the apparent Young's modulus E_s corresponding to the span/depth ratio h/l was calculated by the following equation:

$$E_s = \frac{l^3}{48I}\frac{\Delta P}{\Delta\delta} = \frac{l^3}{4bh^3}\frac{\Delta P}{\Delta\delta} \tag{12}$$

where $\Delta P/\Delta\delta$ is the initial inclination of the load-deflection diagram. Young's modulus E_x and the shear modulus G_{xy} were calculated by regressing the $1/E_s$–$(h/l)^2$ relation into the following equation by the method of least squares.[5–7,9,10]

$$\frac{1}{E_s} = \frac{1}{E_x} + \frac{s}{G_{xy}}\left(\frac{h}{l}\right)^2 \tag{13}$$

Flexural vibration tests

Prior to the static bending tests, Young's and shear moduli were obtained by the flexural vibration tests. The specimen was suspended by two threads at the nodal positions of the free-free vibration corresponding to its resonance mode and was excited in the direction of the depth at one end by a hammer. The resonance frequencies whose mode was from first to fourth were measured by the fast Fourier transform (FFT) digital signal analyzer; and Young's modulus and the shear modulus were obtained from the Timoshenko-Goens-Hearmon method whose details were described in several previous papers.[11] The values obtained were compared with those obtained by the static bending tests mentioned above.

Finite element analyses

Asymmetric four-point and three-point bending tests were simulated by the finite element method (FEM), and the calculated results were compared with those obtained from the asymmetric and three-point bending tests.

The program used was "ISAS-II," which is a library program of the Computer Center of The University of Tokyo. Figure 3 shows the finite element mesh and the boundary conditions used here. The finite elements were divided by the dimensions of 5mm length and 1.25mm depth; the breadth of the element was 20mm. The elastic constants used in the simulations were defined as E_x and E_y for

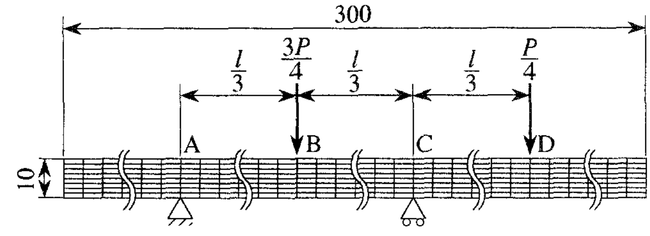

(a) Asymmetric bending

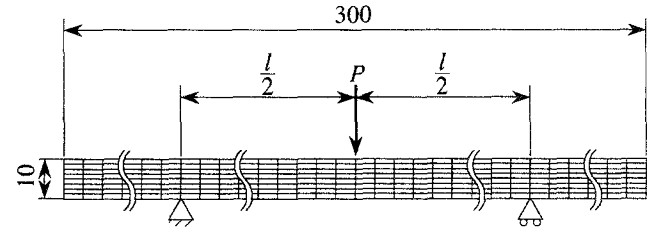

(b) Three-point bending

Fig. 3. Finite element meshes used in the numerical calculations. Meshes are uniformly divided to the dimensions of 5.0 × 1.25mm

Young's moduli in the length and depth directions, G_{xy} for the shear modulus, and ν_{xy} for Poisson's ratio; the values of these constants were E_x = 10GPa, $E_y = G_{xy}$ = 1.2GPa, and ν_{xy} = 0.4. The outer-span length l varied as 90, 120, 150, 180, 210, and 300mm. For the asymmetric bending simulations, loads of 3N and 1N were applied at the top of points B and D in Fig. 3a, respectively. The deflection δ was measured at the bottom of point B. The load-deflection relation was substituted into Eq. (10), and the apparent Young's modulus E_s corresponding to the depth/span ratio h/l was obtained. For the three-point bending simulations, a load of 4N was applied at the top of the center of the beam, and the deflection was measured at the point behind the loading point. The apparent Young's modulus E_s corresponding to the depth/span ratio h/l was obtained by substituting the load-deflection relation into Eq. (12). The simulation results were compared with those obtained from the static bending tests.

Results and discussion

Figure 4 shows the $1/E_s$–$(h/l)^2$ relations for the asymmetric four-point and three-point bending simulations by the finite element method. As mentioned above, the influence of the depth/span ratio was more significant in the asymmetric bending test than in the three-point bending test. According to the bending theory, the inclination of the $1/E_s$–$(h/l)^2$ relation for asymmetric bending is 4.5 times that for three-point bending. From the numerical calculations, the inclination for asymmetric bending was 4.9 times that for three-point bending. Young's modulus E_x and the shear modulus G_{xy}

were calculated by regressing the numberical calculation results into Eqs. (11) and (13). The value of E_x was 11.1 GPa for asymmetric bending and 11.0 for three-point bending. When Timoshenko's shear factor s was determined as 1.2, the value of G_{xy} was derived as 1.22 GPa for asymmetric bending, whereas it was 1.34 GPa for three-point bending. We thought that the validity of Timoshenko's bending theory for asymmetric bending would be verified by these simulation results.

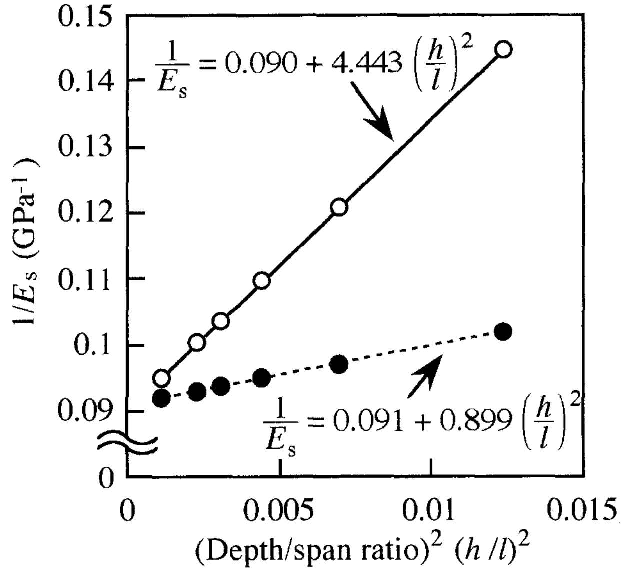

Fig. 4. Value of $1/E_s$ corresponding to the (depth/span ratio)^2 obtained by the finite element method. *Open* and *filled circles* are obtained from the simulations of asymmetric four-point and three-point bending tests, respectively; and *solid* and *dashed lines* are obtained from the regressions of the $1/E_s$–$(h/l)^2$ relations of asymmetric and three-point bending simulations, respectively, into linear relations

Tables 1 and 2 are Young's modulus E_x and the shear modulus G_{xy}, respectively, obtained by the flexural vibration, asymmetric four-point bending, and three-point bending tests. Differently from the finite element calculations, the shear modulus coincided well with that obtained by the vibration test when Timoshenko's shear factor of 1.5 was used. With the bending tests, nonlinear deformation caused by frictional forces and stress concentrations around the loading and supporting points, which cannot be predicted by linear finite element analysis, produced the extra deflection; and the shear modulus calculated using $s = 1.2$ was small. Thus, Timoshenko's shear factor of 1.5 might be applicable to the experimental data. As for three-point bending, the shear moduli could not be obtained properly despite the proper values of Young's moduli. For asymmetric four-point bending, we thought that Young's and shear moduli were properly determined when the depth of the specimen was 5 mm, although the shear modulus of akamatsu was somewhat smaller than that obtained by the vibration tests. Figure 5 shows the inverse value of apparent Young's modulus $1/E_s$ corresponding to the squares of the depth/span ratio $(h/l)^2$ obtained from the asymmetric four-point and three-point bending tests. With three-point bending, the deflection caused by the shearing force is relatively small. For akamatsu with a thickness of 5 mm, this deflection was too small to vary the apparent Young's modulus by the depth/span ratio, and the shear modulus tended to be evaluated as extremely large. For the other results of three-point bending tests, the extra deflection caused by the stress concentration was not reduced effectively, and the shear modulus was evaluated to be small. In contrast, this extra

Table 1. Young's modulus obtained by each method

Depth (mm)	Vibration test (GPa)	Static bending test (GPa)	
		Asymmetric four-point	Three-point
Akamatsu			
5	17.3 ± 1.4	18.3 ± 1.4	18.0 ± 1.1
10		23.3 ± 4.9	16.9 ± 1.6
Shioji			
5	13.4 ± 1.1	13.8 ± 1.8	13.0 ± 2.1
10		16.8 ± 1.5	13.7 ± 1.3

Results are averages ± standard deviation

Table 2. Shear modulus obtained by each method

Depth (mm)	Vibration test (GPa)	Static bending test (GPa)	
		Asymmetric four-point	Three-point
Akamatsu			
5	1.25 ± 0.14	1.07 ± 0.13	4.70 ± 2.06
10		0.56 ± 0.17	0.82 ± 0.03
Shioji			
5	0.91 ± 0.11	0.89 ± 0.25	0.26 ± 0.06
10		0.56 ± 0.11	0.44 ± 0.06

Results are averages ± standard deviation

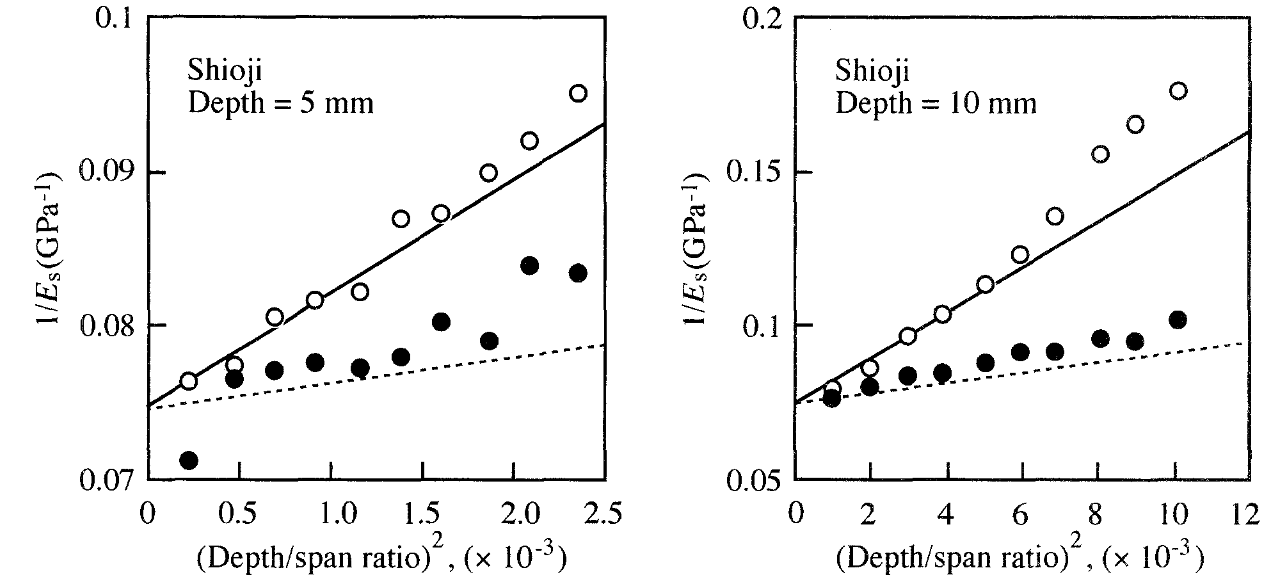

Fig. 5. Examples of the inverse values of apparent Young's moduli corresponding to the squares of depth/span ratios. Blank and solid circles are obtained from the asymmetric four-point and three-point bending tests, respectively. *Solid* and *dashed lines* were obtained by substituting Young's and shear moduli given by the flexural vibration tests into the Timoshenko's bending equations for the asymmetric four-point and three-point bendings, respectively

deflection was effectively obscured with asymmetric four-point bending when the specimen had a small depth/span ratio. Nevertheless, it was significant with an increasing depth/span ratio. As shown in Fig. 5, the $1/E_s$–$(h/l)^2$ relation obtained by the asymmetric bending tests of the specimens with a depth of 10 mm was concave; and the intercept of this relation, which equals $1/E_x$, was evaluated as small, whereas the slope, which corresponds to $4.5s/G_{xy}$, was evaluated as large. We thought this concave tendency was due to the indentations at the loading and supporting points. By reducing these indentations, the depth/span ratio range where Young's and shear moduli are effectively measured would be wider than the experimental results. Nevertheless, plural displacement gauges should be used, complicating the measurement method.

This method is effective for homogeneous material, and there is a concern that it cannot be applied to a large specimen in which inhomogeneity such as knots, grain inclination, and variation of annual ring width are contained. The applicability should be examined for the material with these inhomogeneities. When the method adopted here is undertaken using a homogeneous specimen, however, we recommend that the span is larger than 20 times the depth. The shear modulus can then be obtained effectively by the asymmetric four-point bending tests as can Young's modulus.

Conclusion

We conducted asymmetric four-point bending tests of wood and concluded that the shear modulus can be properly obtained by the asymmetric four-point bending tests when the span is 20 times larger than the depth.

Acknowledgment We thank Prof. Masamitsu Ohta at The University of Tokyo for his advice in writing this article.

References

1. Kon T (1948) The comparative study upon the modulus of rigidity of wood by the methods of compression and torsion. Bull Hokkaido Univ Dept Eng 1:144–156
2. Yoshihara H, Ohta M (1993) Measurement of the shear moduli of wood by the torsion of a rectangular bar. Mokuzai Gakkaishi 39:1993–997
3. Yoshihara H, Ohsaki H, Kubojima Y, Ohta M (1999) Applicability of the Iosipescu shear test on the measurement of the shear properties of wood. J Wood Sci 45:24–29
4. Dumail JF, Olofsson K, Salmén L (2000) An analysis of rolling shear of spruce wood by the Iosipescu method. Holzforschung 54:420–426
5. Yoshihara H, Kubojima Y, Nagaoka K, Ohta M (1998) Measurement of the shear modulus of wood by static bending tests. J Wood Sci 44:15–20
6. Yoshihara H, Ohta M (1998) Feasibility of Timoshenko's bending theory on the measurement of shear modulus of wood. Mem Fac Sci Eng Shimane Univ Ser A 32:177–184
7. Yoshihara H, Fukuda A (1998) Influence of loading point on the static bending test of wood. J Wood Sci 44:473–481
8. Timoshenko SP (1955) Strength of materials. Part 1. Elementary theory and problems, 3rd edn. Van Nostrand, New York, pp 165–310
9. Wangaad FF (1964) Elastic deflection of wood-fiberglass composite beams. For Prod J 14: 256–260
10. Biblis EJ (1965) Shear deflection of wood beams. For Prod J 15:492–498
11. Hearmon RFS (1958) The influence of shear and rotatory inertia on the free flexural vibration of wooden beams. Br J Appl Phys 9:381–388